Journal of the Korean Society of Remote Sensing, Vol.16, No.4, 2000, pp.355~365

Detection of a Point Target Movement with SAR Interferometry

Jung-Hee Jun* and Min-Ho Ka**

Agency for Defence Development*, Dept. of Electrical and Electronic Eng., Yonsei University**

Abstract : The interferometric correlation, or coherence, is calculated to measure the variance of the interferometric phase and amplitude within the neighbourhood of any location within the image as a result of SAR (Synthetic Aperture Radar) interferometric process which utilizes the phase information of the images. The coherence contains additional information that is useful for detecting point targets which change their location in an area of interest (AOI). In this research, a RGB colour composite image was generated with a intensity image (master image), a intensity change image as a difference between master image and slave image, and a coherence image generated as a part of SAR interferometric processing. We developed a technique performing detection of a point target movement using SAR interferometry and applied it to suitable tandem pair images of ERS-1 and ERS-2 as test data. The possibility of change detection of a point target in the AOI could be identified with the technique proposed in this research.

Key Words : SAR, Point Target, Detection, Interferometry, ERS, Tandem.

1. Introduction

SAR interferometry has become an effective technique for the generation of the three-dimensional locations of points within an image, allowing the derivation of topographic maps. In this technique, the interferometric phase is used as a measure of the path length difference between two images (an interferometric pair) acquired from slightly different sensor positions (Li and Goldstein, 1990). As is well known in the interferometric process, the interferometric correlation, or coherence, decreases when there are variations between the two images due, for example, to increasing volume scattering, which is a random process, and to temporal changes, etc (Zebker and John, 1992; Baskakov and Ka, 2000). Therefore, the coherence contains additional information that is useful for applications such as to detect a point target disappeared or appeared in the AOI. This research concerns with the result of performing change detection analyses on a suitable tandem pair images of ERS-1 and ERS-2 over Seoul area as test data using SAR

Received 20 September 2000; Accepted 25 November 2000.

interferometry. Fig. 1 shows a flow of image data processing, which we applied in this study, for change detection of a point target with SAR interferometry. The following Sections 2 and 3 explain the procedure of this data processing flow, Section 4 describes the detection algorithm, techniques and experimental results, and Section 5 summarizes the results.

2. Generation of Coherence Image

For SAR interferometry, two or three image data sets of the same sensor (or at least two with identical specifications) are required. The complex SAR image values represent the intensity and phase of the total backscattering within a resolution element. To compute the interferogram, which is a map of the phase difference between the two images, the two images are coregistered to an accuracy, which is dependent on application, better than, in case of our study, one-eighth of a pixel. The coregistration is performed to maximise the amplitude of the complex correlation coefficient between the imagery, defined as (Rodriguez and Martin, 1992; Jan *et al.*, 1995):

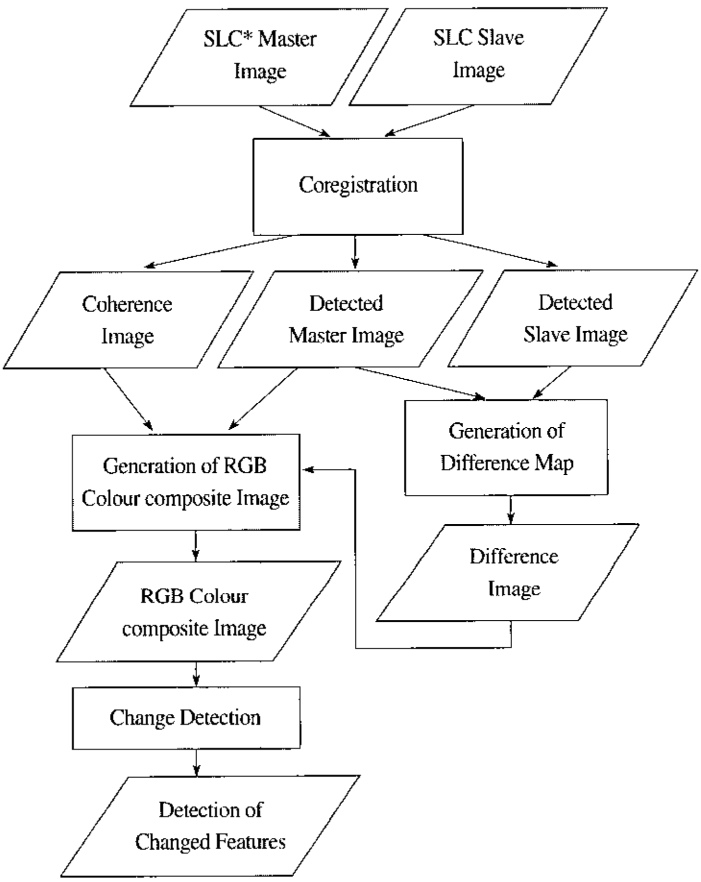

Fig. 1. Flow of image data processing for the detection of a target with SAR interferometry.

$$\gamma = \frac{|E\{s_1 s_2^*\}|}{\sqrt{E\{|s_1|^2\}E\{|s_2|^2\}}} \qquad (1)$$

where s_1 and s_2 are the complex image values, E{} stand for the ensemble average and * represents complex conjugation.

Estimates for the ensemble averages are found by coherently averaging the complex values of N single look pixels:

$$E\{s_1 s_2^*\} = \frac{1}{N}\sum_{i=1}^{N} s_{1,i} s_{2,i}^* \qquad (2)$$

As long as there is partial coherence between the two images, interference phenomena such as fringes are observed. The phase of γ is the interferometric phase and the magnitude of γ is the degree of coherence of s_1 and s_2 and corresponds to values in the range [0, 1].

In this study for the case of ERS, a 5-look interferogram (averaging in azimuth direction, $N = 5$) is computed. The interferometric phase trend of a flat surface or a spherical earth model is subtracted. This step is absolutely necessary for an accurate phase and coherence estimation. As a result of interferometric signal processing, we obtain the normalised interferogram. The magnitude of the normalised interferogram is called interferometric correlation, that is coherence image, and depends on the data processing applied and on the averaging window size used.

The interferometric correlation depends on instrument parameters (wavelength, signal-to-noise ratio, range resolution, number of independent looks) and on parameters related to the geometry (baseline, incidence angle). Volume scattering and temporal changes such as movement of scatterers (wind effects, growth, loss of foliage) or targets of interest and variations in the dielectric constant (freezing, drying) decrease the correlation. Therefore, we can identify temporal changes throughout analyses of a number of sources for decorrelation using the generated interferometric correlation.

3. Data Preparation

AMI (Active Microwave Instrument) of ERS-1 and ERS-2 are coherent SAR sensors measuring both magnitude and phase of the backscattered signal. They are operated at the same function and situation, that is, at 5.3 GHz, VV-polarisation, at 23° of incidence angle (that is, 19° at near range and 27° at far range) (John and Robert, 1991). Furthermore, the orbits have been configured such that an area acquired by ERS-1 can be imaged by ERS-2 one day later. This is known as tandem data and is mainly used for interferometry as the temporal decorrelation is minimised. For this experiment, two tandem image data sets of Seoul (and Inchon area) were selected and ordered as SLC products: the ERS-1 image was acquired on December 21, 1995 and the ERS-2 image was acquired on December 22, 1995 - for future reference, we will refer to the ERS-2 image as master image and the ERS-1 image as slave image. Each image covers an area of 100km 100km on the ground. We established an AOI in master image of approximately 45km (range) × 40km (azimuth) which had areas that were clearly urban, agriculture, mountainous and water like river and interferometric processing was performed using the Earthview INSAR® software package which allowed us to generate a interferometric coherence image and a detected master image and a detected slave image.

Next, we generated a difference image that summarised the intensity change between the detected master image and the detected slave image through the subtraction of the two. For further analyses it was important to generate a 3 band image containing the following layers - master image, difference image (intensity difference between master and slave images) and coherence image. In order to stack these images, we needed to transform these images to the same data type. This is important as the coherence image is output as 8-bit, the master as 16-bit and the difference as 32-bit in case of ERS-1/2. The data conversion and stacking was performed using the ERDAS IMAGINE® image data processing tool and the stacked image is shown in Fig. 2 as an RGB colour composite of the interferometric coherence image (red), the master image (green), and the difference image (blue). This 3 band RGB colour composite image allows to distinguish differences between two images. Thus we could identify the changed features using this 3 band image data. Also, we generated another 3 band RGB colour composite image where we simply exchanged the master image to the slave image for the comparison of change detection and regenerated a difference image with roles reversed.

4. Detection Algorithm with SAR Interferometry

In general, it is not easy to detect point targets changing their locations between two images,

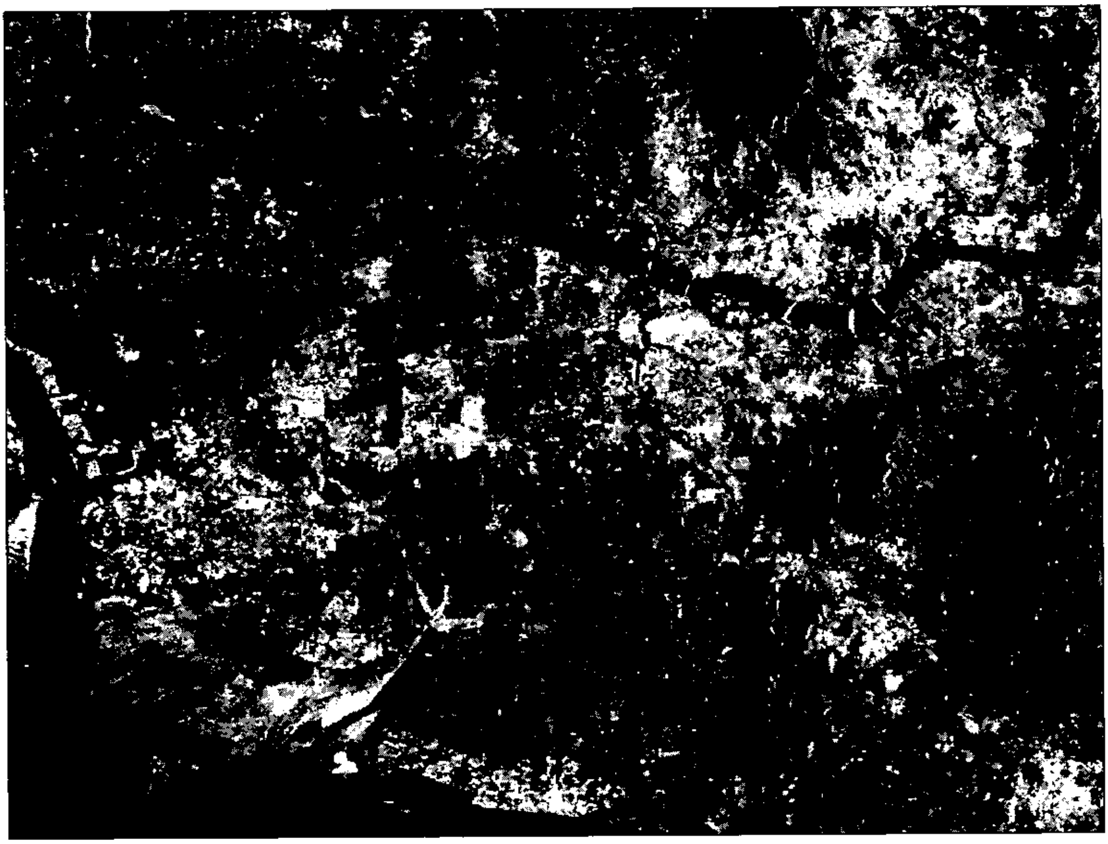

Fig. 2. RGB colour composite image of Seoul and Inchon area with SAR interferometry.

especially on low-resolution ERS images, but the RGB colour composite images generated by SAR interferometry described above allow us to identify targets changed, compared with the approaches based on intensity alone. Therefore, we determined to examine the changes using the interferometric RGB colour composite image of test area of Seoul. On the generated RGB colour composite image, we analysed the colour of the features in great detail. All the features on this image are relate to the characteristics of the coherence, the backscatter intensity, and the backscatter intensity change. Any change of these characteristics results in a change of the colour of the features directly. Thus we can find out whether some targets are subject to change their location with time.

It is not always possible to assign colour directly to a feature or a changed feature as there are so many variations over the image relating to ground conditions, sensor performance, and sensor location at the acquisition time of image. But under the assumption of the same ground conditions and the same sensor performance, we can define 8 possible cases, as we defined in Table 1, which are combinations of whether the coherence value is high or not, whether the intensity is high or not, and whether the intensity change is high or not. The assumption is acceptable for this application because the image acquisition time interval is only one day, and the SAR sensors of ERS-1 and 2 have the same electrical characteristics and imaging mode. These tandem pair images of ERS-1 and ERS-2 are the best choice yet for this kind of application among the existing SAR systems.

From our assumption and definition described in Table 1, we could find distinguishable characteristics of each case. The cases listed in Table 1 are as follows:

- CASE 1 - A permanent feature having a high backscatter intensity in the master image and low in the slave due to the ground conditions, the slight difference of the incidence angle etc. Existing point targets are included in this case. The colour of this feature has yellow and red colour around its position. Fig. 3 is shown as an example of this case.
- CASE 2 - A permanent feature having a high backscatter intensity in the master image but has a higher value in the slave due to the ground conditions, the slight difference of the incidence angle etc. Existing point targets are included in this case. The characteristics of the colour of this feature has red colour around its position. Fig. 4 is shown as an example of this

Table 1. Basic cases of RGB colour composites of the features.

Coherence (Red)	Backscatter Intensity (Green)	Intensity Change (Blue)	Case No.	Colour	Possibility of Change
High	High	High	Case 1	White	Low
High	High	Low	Case 2	Yellow	Low
High	Low	High	Case 3	Violet	Low
High	Low	Low	Case 4	Red	Low
Low	High	High	Case 5	Cyan	High
Low	High	Low	Case 6	Green	High
Low	Low	High	Case 7	Blue	High
Low	Low	Low	Case 8	Black	High

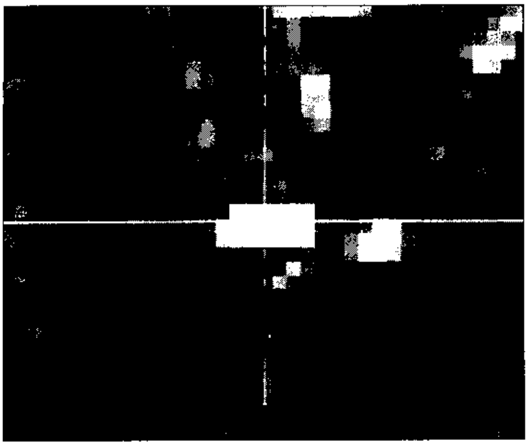

Fig. 3. Case 1: High coherence, high backscatter intensity, high difference.

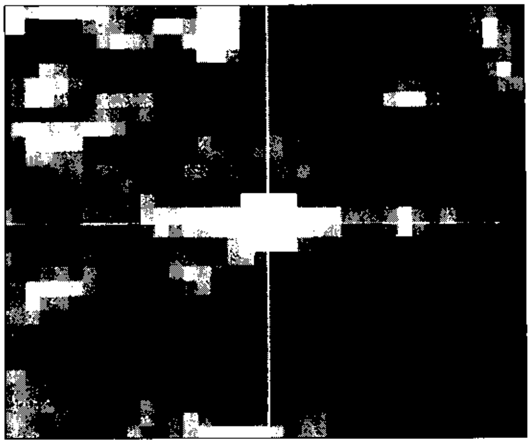

Fig. 4. Case 2: High coherence, high backscatter intensity, low difference.

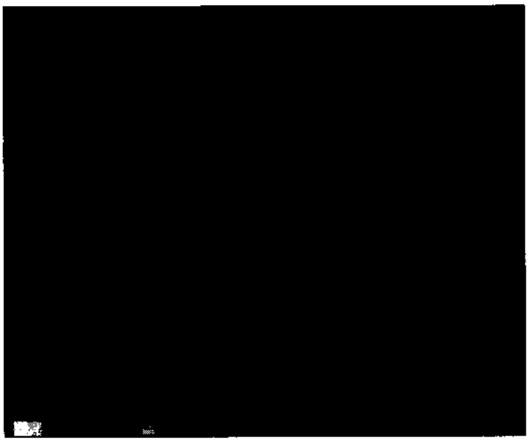

Fig. 5. Case 3: High coherence, low backscatter intensity, high difference.

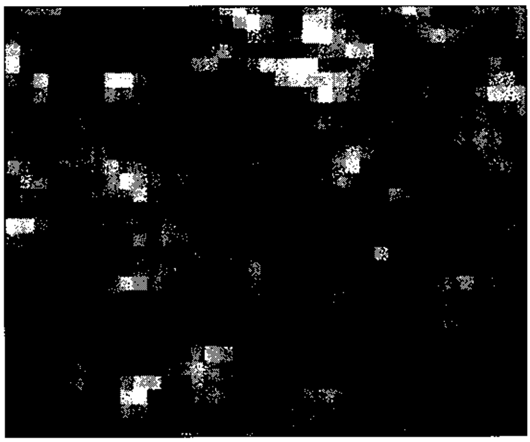

Fig. 6. Case 4: High cohernece, low backscatter intensity, low difference.

case.

- CASE 3 - A permanent feature having a low backscatter in the master and a lower value in the slave due to the ground conditions, the slight difference of the incidence angle etc. This is characteristic of flat unvegetated areas like airports, ports, roads, etc. It is characterised as giving a dark red colour in our experiment due to a possible difference in sensor performance. Fig. 5 is shown as an example.
- CASE 4 - A permanent feature having a low intensity in the master but lower than the slave due to the ground conditions, the slight difference of the incidence angle etc. This is characteristic of flat agriculture areas after cultivation, grassland, etc. Fig. 6 is shown as an example of this case.
- CASE 5 - A feature having a high intensity on the master has disappeared, or has replaced a feature that had a lower intensity on the slave. Newly disappeared features are examples of this case (Fig. 7).
- CASE 6 - A feature having a high intensity on the master has replaced a feature that had a higher

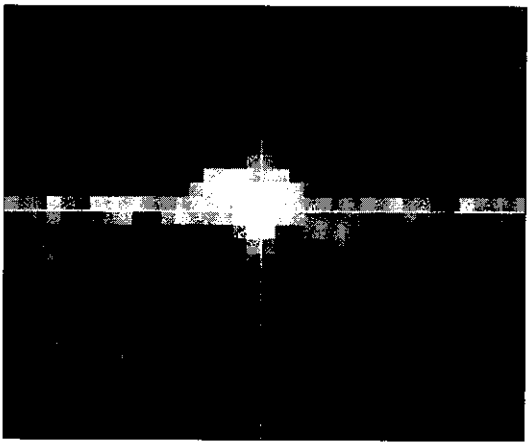

Fig. 7. Case 5: Low cohernece, high backscatter intensity, high difference.

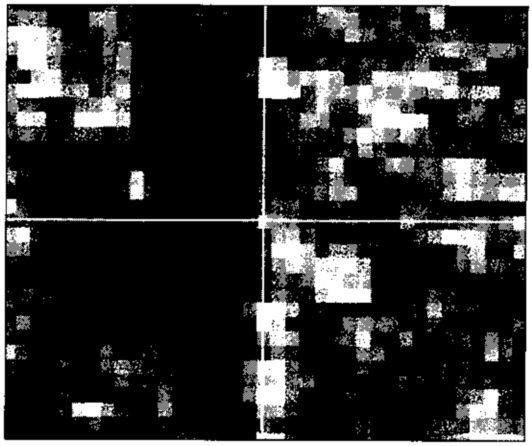

Fig. 8. Case 6: Low cohernece, high backscatter intensity, low difference.

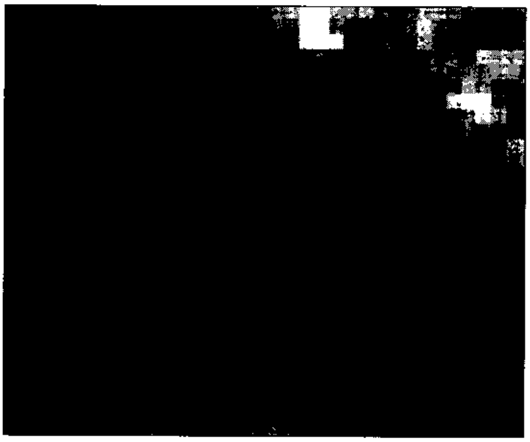

Fig. 9. Case 7: Low coherence, low backscatter intensity, high difference.

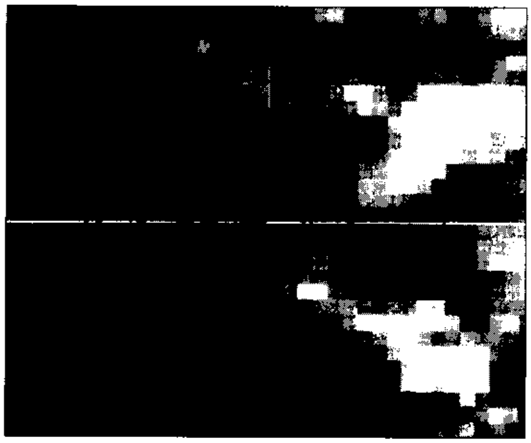

Fig. 10. Case 8: Low coherence, low backscatter intensity, low difference.

intensity on the slave. Newly disappeared features are examples of this case (Fig. 8).

- CASE 7 - A feature having a low intensity on the master has newly appeared or has replaced a feature that had a lower intensity on the slave. Newly appeared features are examples of this case (Fig. 9).
- CASE 8 - A feature on the slave does not appear on the master. Newly detected feature are the example of this case (Fig. 10).

In conclusion, we can find out from these 8 cases that if the pixels have a yellow and/or red colour around it, a change has not occurred, and if the pixels have a black and/or blue colour around that, it means that the target had changed.

Fig. 11 to Fig. 15 illustrate the examples of change detection about the features such as point targets between the master image to the slave image. The number of cases identified in an RGB colour composites may be expanded to as many as necessary, because the RGB colour composite values which stand for the features vary due to ground conditions, weather conditions, sensor performance and sensor location at the acquisition

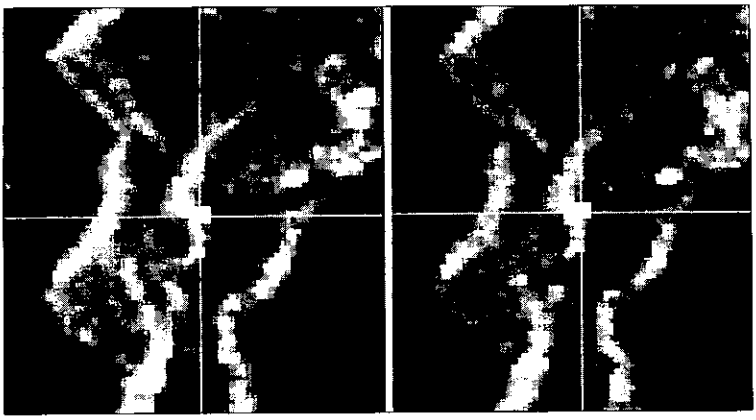

(a) ERS-1: master (b) ERS-2: master

Fig. 11. Example of unchanged feature on the mountain: (a) and (b) - CASE 2.

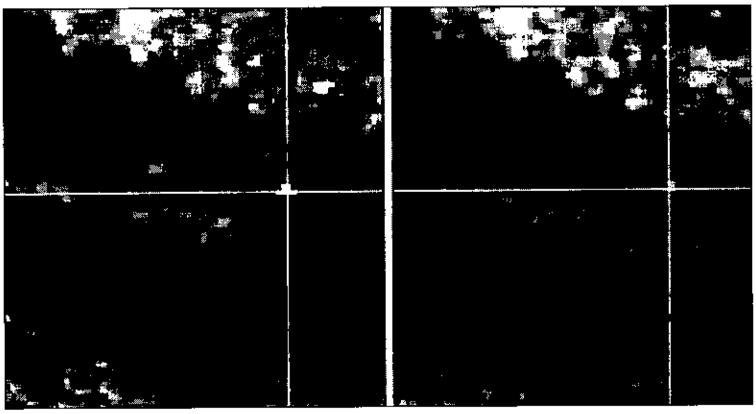

(a) ERS-1: master (b) ERS-2: master

Fig. 12. Example of unchanged feature on the river: (a) - CASE 1; (b) - CASE 2.

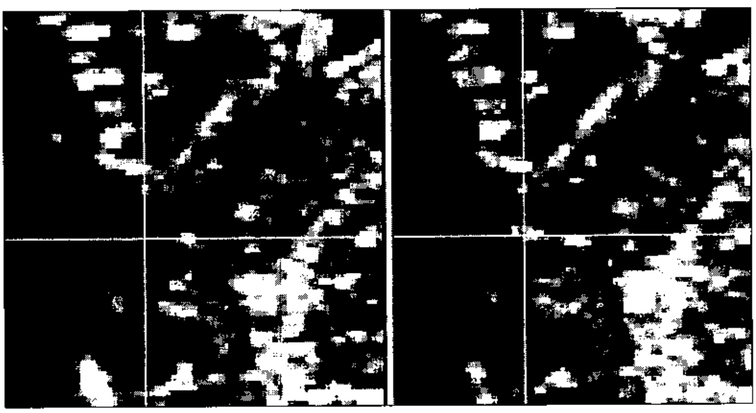

(a) ERS-1: master (b) ERS-2: master

Fig. 13. Example of newly detected feature in the port: (a) - CASE 8; (b) - CASE 7.

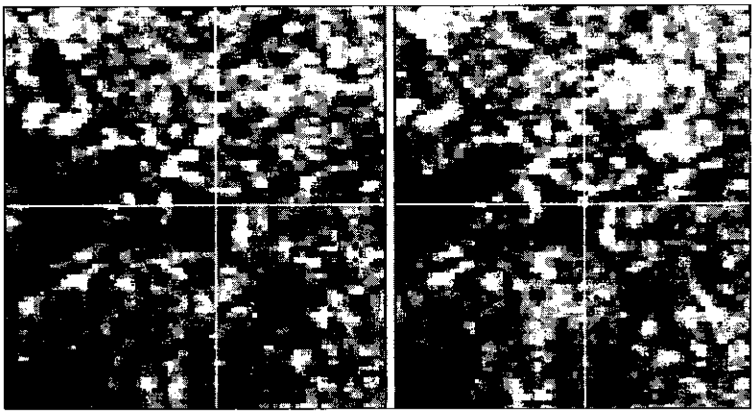

(a) ERS-1: master (b) ERS-2: master

Fig. 14. Example of newly detected feature on the road: (a) - CASE 8; (b) - CASE 7.

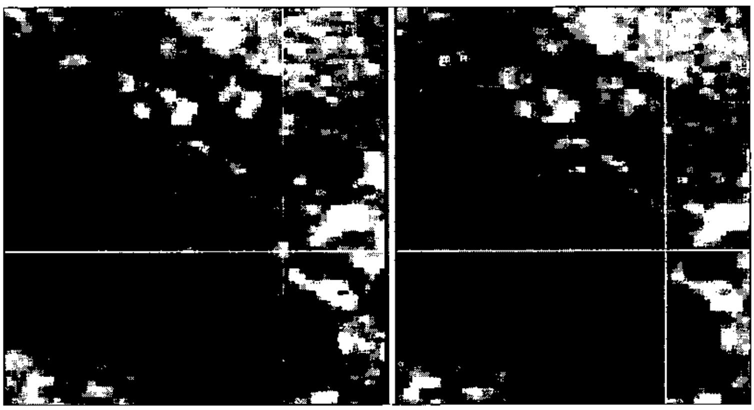

(a) ERS-1: master (b) ERS-2: master

Fig. 15. Example of disappeared feature in the airport: (a) - CASE 7; (b) CASE 6.

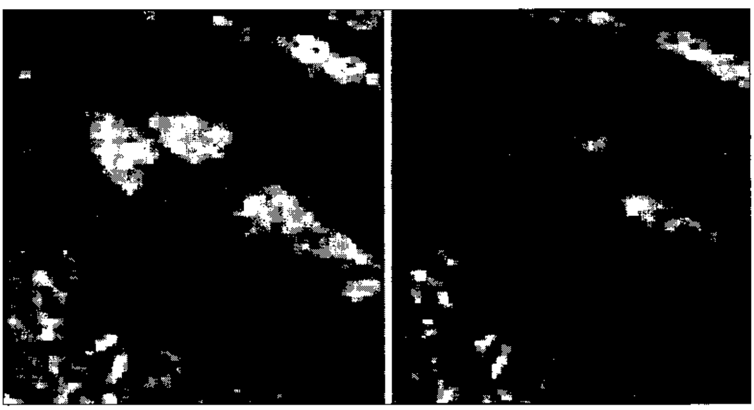

(a) A case of master(ERS-1) slave(ERS-2) (b) A case of slave(ERS-1) master(ERS-2)

Fig. 16. Variety of image colour due to the difference of backscattering intensity.

time of image. If the average intensity of the master image is greater than that of the slave image, the RGB colour composite will become brighter (such as yellow and cyan) generally. If the average intensity of the master image is less than that of the slave image, the RGB colour composite will be darker (such as violet). Thus, we need to perform the change detection whilst recognising this difference. Fig. 16 shows an example of this case. Because the average intensity of the ERS-2 image is approximately 10% greater than that of the ERS-1 image, one RGB colour composite image (right-hand side) has more bright colours when the ERS-2 image is the master, so that urban areas are shown as cyan and good coherence areas such as the agriculture fields are bright red with yellow. The other image (left-hand side) has lower colour levels when the ERS-1 image is the master, so that the urban areas are shown to be green and the good coherence areas are dark red with violet.

5. Conclusions

We generated a RGB colour composite image with a intensity image (master image), a intensity change image as a intensity difference between master image and slave image, and a coherence image generated as a part of SAR interferometry. It contains additional information that has been shown to be useful for detection application. Thus it is possible to detect the point targets which changes their location between the imaging interval such as one day for ERS-1 and 2 tandem case. The time interval of acquiring images over the AOI should not be long in order not to lose the coherency between the images. If the coherence is low over all the pixels of the image due to the long time interval, then we can not distinguish whether the change is due to the movement of a target or temporal decorrelation. So, short time interval between the tandem pair images is the necessary condition for this application.

We have demonstrated that an RGB colour composite image generated with SAR interferometry is an effective way of gaining information about change detection of a point target. More generally, it may be said that the contents and the status of changing features in an image could be identified. Therefore we can state that change detection of a point target by SAR interferometry was feasible in that we could distinguish a number of distinct characteristics over the targets. Throughout the experiment for change detection of a point target, it may be concluded that the contents and the status of changed targets on the image could be identified not only by its pixel intensity but also by phase information of each pixel, using the interferometry technique proposed in this research.

Acknowledgement

This research has been performed jointly by ADD (Agency for Defence Development) and MMS (Matra Marconi Space), UK.

References

Li K. Fuk and Goldstein R. M., 1990, Studies of multibaseline spaceborne interferometric synthetic aperture radars, *IEEE Trans. Geosci. Remote Sens.*, 28(1): 88-97.

Zebker H. A., John Villasennor, 1992, Decorrelation in interferometric radar echos, *IEEE Trans. Geosci. Remote Sens.*, 30(5): 950-959.

Baskakov A. I. and Ka Min Ho, 2000, Analysis of the effect of phase noise on the accuracy characteristics of the interferometric fixed-baseline SAR, *Earth Observation and Remote Sensing*, Harwood Academic, 16(2): 247-256.

Rodriguez E., Martin J. M., 1992, Theory and design of interferometric synthetic aperture radars, *IEEE Proceeding*, part F, 139(2): 147-159.

Jan. O. Hagberg, Lars M. H. and Jan Askne 1995, Repeat-pass SAR interferometry over forested terrain, *IEEE Trans. Geosci. Remote Sens.*, 33(2): 331-340.

John C. Curlander and Robert N. McDonough, 1991, *Synthetic aperture radar: System & Signal processing*, John Whiley & Sons.